Geometry of a qubit

Maris Ozols
(ID 20286921)

December 22, 2007

1 Introduction

Initially my plan was to write about geometry of quantum states of an n-level quantum system. When I was about to finish the qubit case, I realized that I will not be able to cover the remaining part ($n \geq 3$) in a reasonable amount of time. Therefore the generalized Bloch sphere part is completely omitted and I will discuss only the qubit. I will also avoid discussing mixed states.

In general a good reference for this topic is the recent book [1]. Some of the material here is a part of my research – I will indicate it with a star*. All pictures I made myself using *Mathematica*.

The aim of this essay is to convince the reader that despite the fact that quantum states live in a very strange projective Hilbert space, it is possible to speak of its geometry and even visualize some of its aspects.

2 Complex projective space

A *pure state* of an *n-level quantum system* is a vector $|\psi\rangle$ in $\mathbb{C}^n$. It is common to normalize it so that $|\langle\psi|\psi\rangle|^2 = 1$, thus one can think of $|\psi\rangle$ as a *unit vector*. Since the *phase factor* $e^{i\phi}$ ($\phi \in \mathbb{R}$) can not be observed, vectors $|\psi\rangle$ and $e^{i\phi}|\psi\rangle$ correspond to the same physical state.

We can capture both conventions by introducing an equivalence relation

$$\psi \sim \psi' \Leftrightarrow \psi = c\psi' \text{ for some nonzero } c \in \mathbb{C},$$

where ψ and ψ' are nonzero vectors in $\mathbb{C}^n$. One can think of each equivalence class as a "complex" line through the origin in $\mathbb{C}^n$. These lines form a *complex projective space* $\mathbb{C}\mathrm{P}^{n-1}$ (superscript $n-1$ stands for the *complex dimension* of the space). There is a one-to-one correspondence between points in $\mathbb{C}\mathrm{P}^{n-1}$ and physical states of an n-level quantum system.

Unfortunately this description does not make us understand the complex projective space. All we can do is to use the analogy with *real projective space* $\mathbb{R}\mathrm{P}^{n-1}$ (here $n-1$ stands for the real dimension).

For example, if we perform the above construction in $\mathbb{R}^3$, we obtain *real projective plane* $\mathbb{R}\mathrm{P}^2$. One can think of a "point" in $\mathbb{R}\mathrm{P}^2$ as a line through the origin in $\mathbb{R}^3$. We can generalize this idea by saying that a "line" in $\mathbb{R}\mathrm{P}^2$ is a plane through the origin in $\mathbb{R}^3$.

If we restrict our attention only to the unit sphere S^2 at the origin of $\mathbb{R}^3$, we see that a "point" in $\mathbb{R}\mathrm{P}^2$ corresponds to two antipodal points on the sphere, but a "line" corresponds to a great circle. Thus we can think of real projective plane $\mathbb{R}\mathrm{P}^2$ as the unit sphere S^2 in $\mathbb{R}^3$ with antipodal points identified. This space has a very nice structure:

- every two distinct "lines" (great circles) intersect in exactly one "point" (a pair of antipodal points),
- every two distinct "points" determine a unique "line" (the great circle through the corresponding points),
- there is a duality between "points" and "lines" (consider the plane in $\mathbb{R}^3$ orthogonal to the line determined by two antipodal points).

According to the above discussion, the state space of a single qubit corresponds to the *complex projective line* $\mathbb{C}\mathrm{P}^1$. The remaining part of this essay will be about ways how to visualize it. At first in Sect. 3 I will consider the standard Bloch sphere representation of a qubit and discuss some properties of Pauli matrices. Then I will consider two ways of representing the qubit state with a single complex number. In Sect. 4 the state space will be visualized as a unit disk in the complex plane, but in Sect. 5 – as the extended complex plane $\mathbb{C}_\infty$. Then in Sect. 6 I will discuss the stereographic projection that provides a correspondence between the extended complex plane $\mathbb{C}_\infty$ and the Bloch sphere S^2. I will conclude the essay in Sect. 7 with the discussion of the Hopf fibration of the 3-sphere S^3, that makes the correspondence between $\mathbb{C}\mathrm{P}^1$ and the Bloch sphere S^2 possible. I will also shortly discuss the possibility of using other Hopf fibrations to study the systems of several qubits.

3 Bloch sphere representation

This section is a quick introduction to the standard Bloch sphere representation of a single qubit state. I will begin by defining the Bloch vector, and expressing the qubit density matrix in terms of it. Then I will show how this can be used to express a general 2×2 unitary matrix. I will conclude this section with the discussion of several interesting facts about Pauli matrices.

A pure qubit state $|\psi\rangle$ is a point in $\mathbb{C}\mathrm{P}^1$. The standard convention is to assume that it is a unit vector in $\mathbb{C}^2$ and ignore the global phase. Then without the loss of generality we can write

$$|\psi\rangle = \begin{pmatrix} \cos\frac{\theta}{2} \\ e^{i\varphi}\sin\frac{\theta}{2} \end{pmatrix}, \tag{1}$$

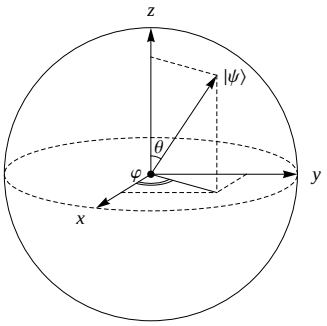

Figure 1: Angles θ and φ of the Bloch vector corresponding to state $|\psi\rangle$.

where $0 \leq \theta \leq \pi$ and $0 \leq \varphi < 2\pi$ (the factor $1/2$ for θ in (1) is chosen so that these ranges resemble the ones for *spherical coordinates*).

For almost all states $|\psi\rangle$ there is a unique way to assign the parameters θ and φ. The only exception are states $|0\rangle$ and $|1\rangle$, that correspond to $\theta = 0$ and $\theta = \pi$ respectively. In both cases φ does not affect the physical state. Note that spherical coordinates with *latitude* θ and *longitude* φ have the same property, namely – the longitude is not defined at poles. This suggests that the state space of a single qubit is topologically a sphere.

3.1 Bloch vector

Indeed, there is a one-to-one correspondence between pure qubit states and the points on a unit sphere S^2 in $\mathbb{R}^3$. This is called *Bloch sphere representation* of a qubit state (see Fig. 1). The *Bloch vector* for state (1) is $\vec{r} = (x, y, z)$, where

$$\begin{cases} x = \sin\theta\cos\varphi, \\ y = \sin\theta\sin\varphi, \\ z = \cos\theta. \end{cases} \tag{2}$$

The *density matrix* of (1) is

$$\rho = |\psi\rangle\langle\psi| = \frac{1}{2}\begin{pmatrix} 1+\cos\theta & e^{-i\varphi}\sin\theta \\ e^{i\varphi}\sin\theta & 1-\cos\theta \end{pmatrix} = \frac{1}{2}\left(I + x\sigma_x + y\sigma_y + z\sigma_z\right), \tag{3}$$

where (x, y, z) are the coordinates of the Bloch vector and

$$I = \begin{pmatrix} 1 & 0 \\ 0 & 1 \end{pmatrix}, \quad \sigma_x = \begin{pmatrix} 0 & 1 \\ 1 & 0 \end{pmatrix}, \quad \sigma_y = \begin{pmatrix} 0 & -i \\ i & 0 \end{pmatrix}, \quad \sigma_z = \begin{pmatrix} 1 & 0 \\ 0 & -1 \end{pmatrix} \tag{4}$$

are called *Pauli matrices*. We can write (3) more concisely as

$$\rho = \frac{1}{2}\left(I + \vec{r}\cdot\vec{\sigma}\right), \quad \vec{r} = (x, y, z), \quad \vec{\sigma} = (\sigma_x, \sigma_y, \sigma_z). \tag{5}$$

If $\vec{r}_1$ and $\vec{r}_2$ are the Bloch vectors of two pure states $|\psi_1\rangle$ and $|\psi_2\rangle$, then

$$|\langle\psi_1|\psi_2\rangle|^2 = \mathrm{Tr}(\rho_1\rho_2) = \frac{1}{2}(1 + \vec{r}_1 \cdot \vec{r}_2). \tag{6}$$

This relates the inner product in $\mathbb{C}^2$ and $\mathbb{R}^3$. Notice that orthogonal quantum states correspond to antipodal points on the Bloch sphere, i.e., if $|\langle\psi_1|\psi_2\rangle|^2 = 0$, then $\vec{r}_1 \cdot \vec{r}_2 = -1$ and hence $\vec{r}_1 = -\vec{r}_2$.

3.2 General 2×2 unitary*

A useful application of the Bloch sphere representation is the expression for a general 2×2 unitary matrix. I have seen several such expressions, but it is usually hard to memorize them or to understand the intuition. I am sure that my way of writing it is definitely covered in some book, but I have not seen one.

To understand the intuition, consider the unitary

$$U = |0\rangle\langle 0| + e^{i\varphi}|1\rangle\langle 1| = \begin{pmatrix} 1 & 0 \\ 0 & e^{i\varphi} \end{pmatrix}. \tag{7}$$

It acts on the basis states as follows:

$$U|0\rangle = |0\rangle, \quad U|1\rangle = e^{i\varphi}|1\rangle. \tag{8}$$

Since U adds only a global phase to $|0\rangle$ and $|1\rangle$, their Bloch vectors $(0, 0, \pm 1)$ must correspond to the axis of rotation of U. To get the angle of rotation, consider how U acts on $|+\rangle$:

$$U\frac{|0\rangle + |1\rangle}{\sqrt{2}} = \frac{|0\rangle + e^{i\varphi}|1\rangle}{\sqrt{2}} = \frac{1}{\sqrt{2}}\begin{pmatrix} 1 \\ e^{i\varphi} \end{pmatrix},$$

which is $|+\rangle$ rotated by an angle φ around z-axis. Notice that (8) just means that $|0\rangle$ and $|1\rangle$ are the eigenvectors of U with eigenvalues 1 and $e^{i\varphi}$.

To write down a general rotation around axis $\vec{r}$ by angle φ, we use the fact that $\vec{r}$ and $-\vec{r}$ correspond to orthogonal quantum states. Then in complete analogy with (7) we write:

$$U(\vec{r}, \varphi) = \rho(\vec{r}) + e^{i\varphi}\rho(-\vec{r}). \tag{9}$$

In fact, this is just the spectral decomposition.

3.3 Pauli matrices

Now let us consider some properties of the Pauli matrices (4) that appeared in the expression (5) of the qubit density matrix.

3.3.1 Finite field of order 4

The first observation is that they form a *group* (up to global phase) under matrix multiplication. For example, $\sigma_x \cdot \sigma_y = i\sigma_z \approx \sigma_z$. This group is isomorphic to $\mathbb{Z}_2 \times \mathbb{Z}_2 = (\{00, 01, 10, 11\}, +)$. However, one can think of it also as the additive group of the *finite field* of order 4:

$$\mathbb{F}_4 = (\{0, 1, \omega, \omega^2\}, +, *), \quad x \equiv -x, \quad \omega^2 \equiv \omega + 1,$$

because the elements of $\mathbb{F}^4$ can be thought as vectors of a two-dimensional vector space with basis $\{1, \omega\}$, where $1 \equiv \left(\begin{smallmatrix}1\\0\end{smallmatrix}\right)$ and $\omega \equiv \left(\begin{smallmatrix}0\\1\end{smallmatrix}\right)$. Then one possible way to define the correspondence between Pauli matrices and $\mathbb{F}_4$ is [2]:

$$(0, 1, \omega, \omega^2) \Longleftrightarrow (I, \sigma_x, \sigma_z, \sigma_y).$$

This is useful when constructing *quantum error correction codes* [2].

3.3.2 Quaternions

If we want to capture the multiplicative properties of Pauli matrices in more detail, then we have to consider the global phase. The set of all possible phases that can be obtained by multiplying Pauli matrices is $\{\pm 1, \pm i\}$. Thus we can get a group of order 16. However, we can get a group of order 8 with the following trick: $(i\sigma_x) \cdot (i\sigma_y) = -(i\sigma_z)$, thus the phases are only ± 1. It turns out that this group is isomorphic to the multiplicative group of *quaternions*:

$$(1, i, j, k) \Longleftrightarrow (I, i\sigma_z, i\sigma_y, i\sigma_x).$$

The laws of quaternion multiplication can be derived from:

$$i^2 = j^2 = k^2 = ijk = -1.$$

3.3.3 Clifford group*

Pauli matrices are elements of a larger group called *Clifford group* or *normalizer group*. In the qubit case it is defined as follows:

$$C = \{U | \sigma \in P \Rightarrow U\sigma U^\dagger \in P\}, \text{ where } P = \{\pm I, \pm\sigma_x, \pm\sigma_y, \pm\sigma_z\}.$$

For example, the *Hadamard gate* $H = \frac{1}{\sqrt{2}}\left(\begin{smallmatrix}1 & 1\\1 & -1\end{smallmatrix}\right)$ is also in this set. One can show that a matrix is in the Clifford group if and only if it corresponds to a rotation of the Bloch sphere that permutes the coordinate axes (both, positive and negative directions). For example, it can send direction x to direction $-z$. There are 6 ways where the first axis can go, and then 4 ways for the second axis – once the first axis is fixed, we can only rotate by $\pi/2$ around it. Hence there are 24 such rotations.

Let us see what they correspond to. Consider the rotation axes corresponding to the vertices of *octahedron*, *cube*, and *cuboctahedron* shown in Fig. 2:

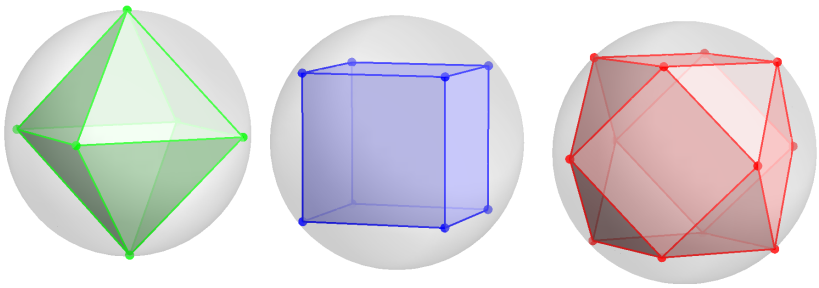

Figure 2: Octahedron, cube, and cuboctahedron.

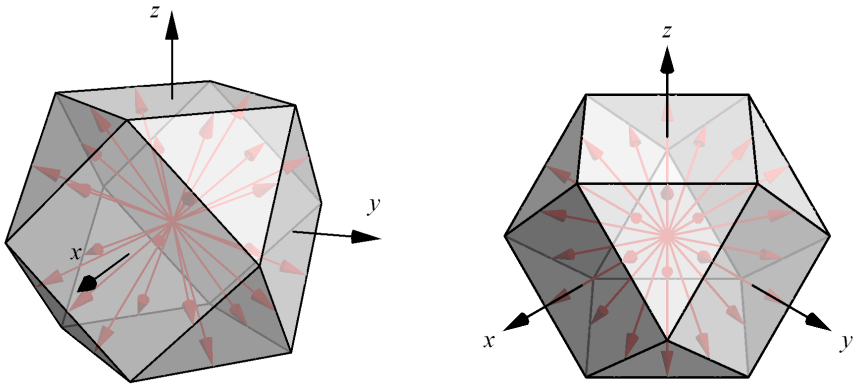

Figure 3: Two views of cuboctahedron. The 24 arrows correspond to the midpoints of its edges. Clifford group operations permute these arrows transitively.

- *Octahedron* has 6 vertices and thus 3 rotation axes (they are the coordinate axes x, y, z). There are 3 possible rotation angles: $\pm\pi/2$ and π. Hence we get $3 \cdot 3 = 9$ rotations. For example, Pauli matrices are of this type, since they correspond to a rotation by π about some coordinate axis.

- *Cube* has 8 vertices and therefore 4 axes. There are only 2 possible angles $\pm 2\pi/3$ giving $4 \cdot 2 = 8$ rotations.

- *Cuboctahedron* has 12 vertices and 6 axes. The only possible angle is π, thus it gives 6 rotations. For example, the Hadamard matrix is of this type (it swaps x and z axis).

If we total, we get 23, plus the identity operation is 24. The unitary matrices for these rotations can be found using (9).

One can observe that all three polyhedra shown in Fig. 2 have the same symmetry group and it has order 24. This group is isomorphic to S_4 – the

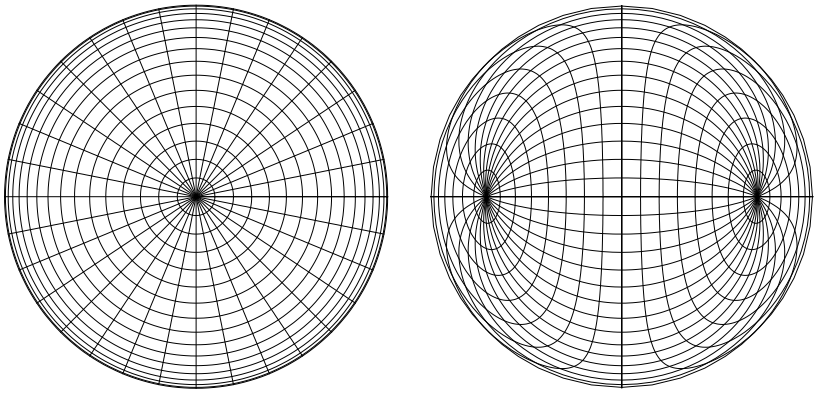

Figure 4: Hadamard transformation H in the unit disk representation. The disks shown correspond to the states $|0\rangle$ and $|+\rangle = H|0\rangle$ respectively.

symmetric group of 4 objects, since the corresponding rotations allow to permute the four diagonals of the cube in arbitrary way.

There is a uniform way of characterizing the three types of rotations described above. Observe that cuboctahedron has exactly 24 edges and there is exactly one way how to take one edge to other, because each edge has a triangle on one side and a square on the other. Therefore the Clifford group consists of exactly those rotations that take one edge of a cuboctahedron to another. This is illustrated in Fig. 3.

4 Unit disk representation*

There is another geometrical interpretation of equation (1). Observe that a pure qubit state $|\psi\rangle = \binom{\alpha}{\beta} \in \mathbb{C}^2$ is completely determined by its second component

$$\beta = e^{i\varphi} \sin \tfrac{\theta}{2}. \tag{10}$$

Since $|\beta| \leq 1$, the set of pure qubit states can be identified with a unit disk in the complex plane (the polar coordinates of β are (r, φ), where $r = \sin \frac{\theta}{2}$). The origin corresponds to $|0\rangle$, but all points on the unit circle $|\beta| = 1$ are identified with $|1\rangle$. The topological interpretation is that we puncture the Bloch sphere at its South pole and flatten it to a unit disk.

As an example of a unitary operation in this representation, consider the action of the Hadamard gate H. The way it transforms the curves of constant θ and φ is shown in Fig. 4. After this transformation the origin corresponds to $|+\rangle$, but the unit circle to $|-\rangle$ state. The states $|1\rangle$ and $|0\rangle$ correspond to the "left pole" and "right pole" respectively.

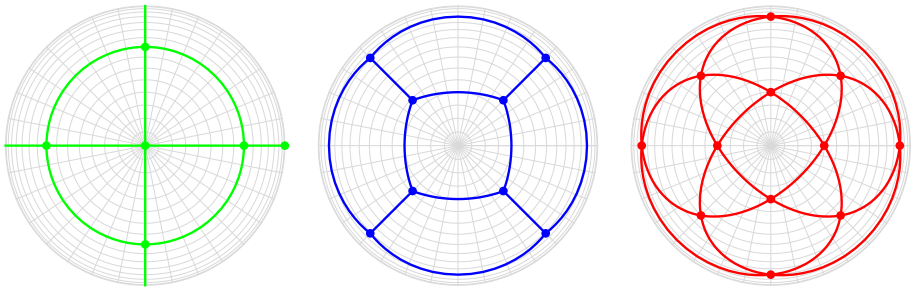

Figure 5: Octahedron, cube, and cuboctahedron in the unit disk representation. Their vertices are the roots of polynomials (11), (12), and (13) respectively.

Another way of interpreting Fig. 4 is to say that the $|0\rangle$ state is show on the left and $|+\rangle = H|0\rangle$ is shown on the right, since in both cases these states correspond to the origin. Then in the image on the right one can clearly see that $|+\rangle = \frac{1}{\sqrt{2}}(|0\rangle + |1\rangle)$ is a superposition of $|0\rangle$ and $|1\rangle$.

The advantage of this representation is that it corresponds to a bounded set in the complex plane and it shows "both sides" of the Bloch sphere. Thus it is useful for drawing pictures of configurations of qubit states (see Fig. 5). It also provides a very concise way to describe the vertices of regular polyhedra [3]. For example, the β coefficients of qubit states corresponding to the vertices of the octahedron, cube, and cuboctahedron are the roots of the following polynomials:

$$\beta(\beta - 1)(4\beta^4 - 1) = 0, \tag{11}$$

$$36\beta^8 + 24\beta^4 + 1 = 0, \tag{12}$$

$$256\beta^{12} - 128\beta^8 - 44\beta^4 + 1 = 0, \tag{13}$$

where the convention that $|1\rangle$ corresponds to $\beta = 1$ is used (see Fig. 5).

5 Extended complex plane representation

There is yet another way how to represent a qubit. It is very similar to the previous one, but has an advantage that unitary operations can be described in a simple way – as *conformal maps* (a map in the complex plane that preserves local angles). However, the state space is not bounded anymore.

This representation of a qubit appeared in the context of quantum computing in [4]. However, it has been known for some time in a different context, namely four-dimensional geometry of *Minkowsky vector space*. Despite the completely different context, I suggest [5, pp. 10] as a very good reference.

To be consistent with Sect. 3 our notation will differ from [4, 5]. Hence the

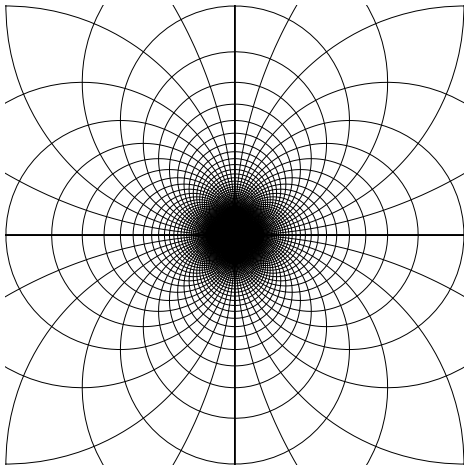

Figure 6: The coordinate grid after the conformal transformation $1/\zeta$ corresponding to the unitary NOT gate σ_x.

geometrical interpretation in the next section will be somewhat awkward. [1]

We used the second component β to identify a pure qubit state $|\psi\rangle = \left(\begin{smallmatrix}\alpha\\ \beta\end{smallmatrix}\right)$ in the previous section. This approach had a deficiency that all points on the unit circle $|\beta| = 1$ correspond to the same state, namely $|1\rangle$. Let us consider a way how to avoid this problem.

Let $\psi = \left(\begin{smallmatrix}\alpha\\ \beta\end{smallmatrix}\right)$ be a non-zero vector in $\mathbb{C}^2$. Then the ratio

$$\zeta = \frac{\alpha}{\beta} \tag{14}$$

uniquely determines the "complex line" through ψ, since all points on the same "line" have equal ζ. To tread the case when $\beta = 0$ we have to extend the complex plane $\mathbb{C}$ by adding a *point at infinity*. The obtained set $\mathbb{C}_\infty = \mathbb{C} \cup \{\infty\}$ is called *extended complex plane*.

For a pure qubit state (1) we have

$$\zeta = e^{-i\varphi} \cot \frac{\theta}{2}. \tag{15}$$

We see that this representation is not redundant, since $|0\rangle$ and $|1\rangle$ correspond to $\zeta = \infty$ and $\zeta = 0$ respectively. Hence (15) provides a one-to-one correspondence between pure qubit states and the points on the extended complex plane $\mathbb{C}_\infty$.

Let $U = \left(\begin{smallmatrix}a & b\\ c & d\end{smallmatrix}\right)$ be a unitary matrix. Then it transforms $|\psi\rangle$ as follows:

$$U|\psi\rangle = \begin{pmatrix} a & b \\ c & d \end{pmatrix} \begin{pmatrix} \alpha \\ \beta \end{pmatrix} = \begin{pmatrix} a\alpha + b\beta \\ c\alpha + d\beta \end{pmatrix}.$$

[1] They use $e^{-i\varphi}$ instead of $e^{i\varphi}$ in (1). Then (18) reads $\zeta = \frac{x+iy}{1-z}$, which corresponds to the stereographic projection from the Bloch sphere to the extended complex plane.

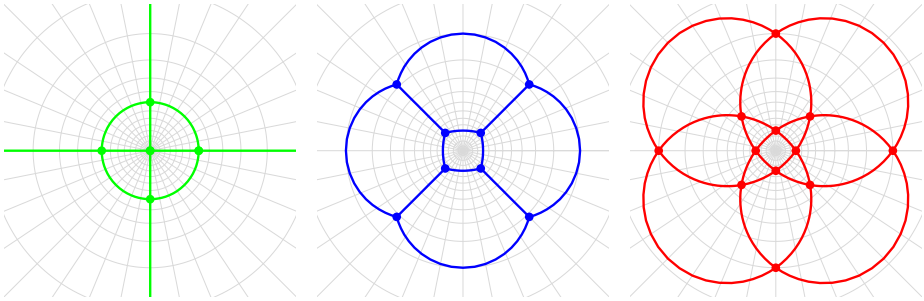

Figure 7: Octahedron, cube, and cuboctahedron in the extended complex plane representation.

Now the new ratio ζ' is[2]

$$\zeta' = \frac{a\alpha + b\beta}{c\alpha + d\beta} = \frac{a\zeta + b}{c\zeta + d}.$$

Thus U corresponds to the following transformation of $\zeta \in \mathbb{C}_\infty$:

$$f(\zeta) = \frac{a\zeta + b}{c\zeta + d}, \tag{16}$$

where the following conventions are used:

$$f\left(-\frac{d}{c}\right) = \infty, \quad f(\infty) = \frac{a}{c}.$$

Since U is unitary, $\det U = ad - bc \neq 0$, hence f is not constant. Such f is a special kind of conformal map called *linear fractional transformation* or *Möbius transformation* [6, pp. 47]. It has some nice properties, for example:

- it transforms circles to circles (line is considered as a "very big" circle),
- a circle can be taken to any other by a Möbius transformation.

The conformal maps for the most common unitary operations are given in Table 1. For example, NOT gate σ_x corresponds to the map $f(\zeta) = 1/\zeta$ that sends 0 to ∞ and vice versa, as expected. The way it transforms the coordinate grid is shown in Fig. 6. The other transformations act similarly.

This representation also can be used to visualize configurations of qubit states, but the result might be more distorted than using unit disk representation (compare Fig. 5 and Fig. 7).

[2]We can divide by zero, since we work in the extended complex plane.

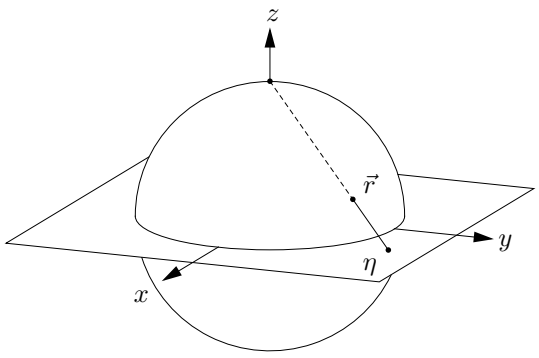

Figure 8: Stereographic projection from the Bloch sphere to the extended complex plane.

6 Stereographic projection

In this section we will see the connection between the Bloch sphere representation discussed in Sect. 3 and the extended complex plane.

Let us define the *stereographic projection* from the Bloch sphere to the xy-plane. To find the projection of a Bloch vector $\vec{r} = (x, y, z)$, consider the line connecting the North pole and $\vec{r}$. Its intersection η with the xy-plane is the projection of $\vec{r}$ (see Fig. 8).

To find the projection η, let us interpret $\vec{r}$ as $(x+iy, z) \in \mathbb{C} \times \mathbb{R} \cong \mathbb{R}^3$. Then η is a positive multiple of $x + iy$. From Fig. 9 we see that $\frac{\eta}{x+iy} = \frac{1}{1-z}$, hence

$$\eta = \frac{x + iy}{1 - z}. \tag{17}$$

Observe that the North pole $\vec{r} = (0, 0, 1)$ projects to $\eta = \infty$. One can verify that ζ defined in (15) is the complex conjugate of η:

$$\zeta = \overline{\eta} = \frac{x - iy}{1 - z}, \tag{18}$$

where (x, y, z) are the coordinates of the Bloch vector (2). Therefore the stereographic projection allows to switch between the two representations.

Now we can understand the geometrical meaning of the definition (15) of ζ. From Fig. 10 one can directly see that the factor $\cot\frac{\theta}{2}$ corresponds to the distance of the projection to the origin or simply the absolute value of ζ.

Unitary gate U	I	σ_x	σ_y	σ_z	H
Conformal map $f(\zeta)$	ζ	$\frac{1}{\zeta}$	$-\frac{1}{\zeta}$	$-\zeta$	$\frac{\zeta+1}{\zeta-1}$

Table 1: The correspondence between unitary operations and conformal maps.

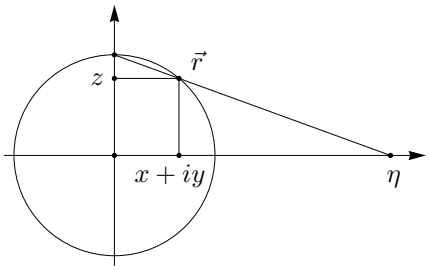

Figure 9: The projection η of the Bloch vector $\vec{r} = (x + iy, z)$ or the geometrical meaning of equation (17).

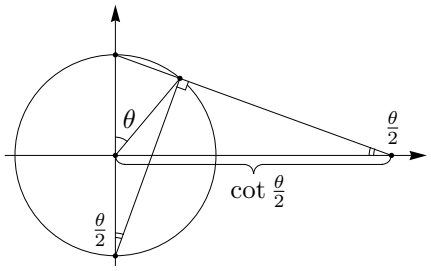

Figure 10: Geometrical interpretation of $\cot\frac{\theta}{2}$ in equation (15).

7 Hopf fibration

The Bloch sphere formalism introduced in Sect. 3 can be stated in a different way – as the *Hopf fibration* of the 3-dimensional sphere S^3 in $\mathbb{R}^4$. For an elementary introduction to this fibration see [7]. I will follow [8, pp. 103]. First I will show that the 3-dimensional sphere S^3 can be thought as a disjoint union of circles S^1. Then I will describe a map from S^3 to S^2 that provides a bijection between these circles and the points on the 2-dimensional Bloch sphere.

7.1 Three-dimensional sphere

Let us identify $\mathbb{R}^4$ and $\mathbb{C}^2$ in the obvious way:

$$\begin{pmatrix} x \\ y \\ z \\ w \end{pmatrix} \cong \begin{pmatrix} x+iy \\ z+iw \end{pmatrix}. \tag{19}$$

Then the unit sphere S^3 can be defined as

$$\mathrm{S}^3 = \left\{ \psi \in \mathbb{C}^2 \middle| \, |\psi| = 1 \right\}.$$

Let $\mu \in \mathbb{C}^2$ be a unit vector ($\mu \in \mathrm{S}^3$). Then the "complex line" in direction μ is

$$L_\mu = \{c\mu | c \in \mathbb{C}\}.$$

Let C_μ be the intersection of L_μ and S^3:

$$C_\mu = L_\mu \cap \mathrm{S}^3 = \left\{ e^{i\varphi}\mu | \varphi \in \mathbb{R} \right\}. \tag{20}$$

Notice that C_μ is a (non-degenerate) circle S^1 on the surface of S^3. Moreover, for each $\mu \in \mathrm{S}^3$ the circle C_μ is uniquely determined and contains μ. Thus one can think of S^3 as a union of circles S^1.

To visualize this, let us introduce the spherical coordinates in $\mathbb{R}^4$ and use the stereographic projection to project S^3 to a more familiar space $\mathbb{R}^3$. In analogy with (2) for $\mathbb{R}^3$, the coordinates of a unit vector $\mu \in \mathbb{R}^4$ can be defined as:

$$\begin{cases} x = \sin\alpha \sin\beta \sin\gamma, \\ y = \sin\alpha \sin\beta \cos\gamma, \\ z = \sin\alpha \cos\beta, \\ w = \cos\alpha, \end{cases} \tag{21}$$

where $\alpha, \beta \in [0, \pi]$ and $\gamma \in [0, 2\pi)$. According to (20) the circle C_μ for $\mu = \left(\begin{smallmatrix} x+iy \\ z+iw \end{smallmatrix}\right)$ explicitly reads as:

$$C_\mu = e^{i\varphi} \begin{pmatrix} x+iy \\ z+iw \end{pmatrix} \cong \begin{pmatrix} \cos\varphi & -\sin\varphi & 0 & 0 \\ \sin\varphi & \cos\varphi & 0 & 0 \\ 0 & 0 & \cos\varphi & -\sin\varphi \\ 0 & 0 & \sin\varphi & \cos\varphi \end{pmatrix} \begin{pmatrix} x \\ y \\ z \\ w \end{pmatrix}. \tag{22}$$

In analogy with the stereographic projection (17) from S^2 to $\mathbb{C}_\infty$ discussed in the previous section, we can generalize it as follows:

$$\begin{pmatrix} x \\ y \\ z \\ w \end{pmatrix} \mapsto \frac{1}{1-w} \begin{pmatrix} x \\ y \\ z \end{pmatrix}. \tag{23}$$

To obtain a picture, it remains to choose a unit vector $\mu \in \mathbb{R}^4$ by putting some α, β, and γ in (21), compute the circle C_μ using (22) and project it to $\mathbb{R}^3$ according to (23). As the result one obtains the space $\mathbb{R}^3$ completely filled with circles in a way that every two of them are linked. The result is shown in Fig. 11 (the vertical line corresponds to the "circle through infinity"). If α and β are fixed, then the circles corresponding to different γ sweep the surface of a *torus*. One such torus is shown in Fig. 12.

7.2 The Hopf map

Now let us see how these circles can be mapped to the points on the Bloch sphere S^2. First let us introduce some basic vocabulary. A *fibre* of a map is the set of points having the same image. For example, the fibres of the projection in $\mathbb{R}^3$ to a plane are the lines orthogonal to that plane (we call this plane *base space*). Since these lines do not overlap and fill the whole space, we say that $\mathbb{R}^3$ is *fibred* by $\mathbb{R}^1$. The common way to denote this is as follows:

$$\text{fibred space} \xrightarrow{\text{fibre}} \text{base space}.$$

In our case this reads as $\mathbb{R}^3 \xrightarrow{\mathbb{R}^1} \mathbb{R}^2$. Since $\mathbb{R}^3 = \mathbb{R}^1 \times \mathbb{R}^2$, our fibration is called *trivial*. The Hopf fibrations are the simplest examples of *non-trivial* fibrations.

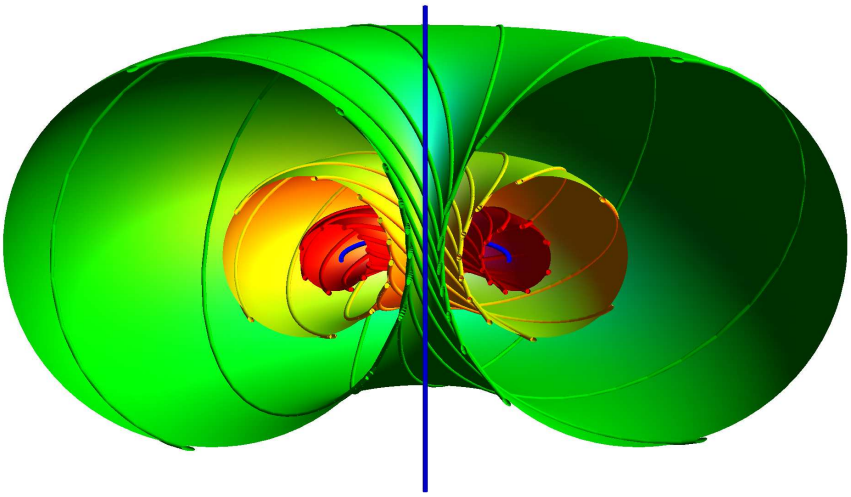

Figure 11: Stereographic projection of the S^3 fibration. The tori correspond to $\alpha = \frac{\pi}{2}$ and $\beta = k\frac{\pi}{8}$, where $k \in \{0, 1, 2, 3, 4\}$. When $k = 0$ or $k = 4$ the tori are degenerate – they correspond to the blue line and circle respectively.

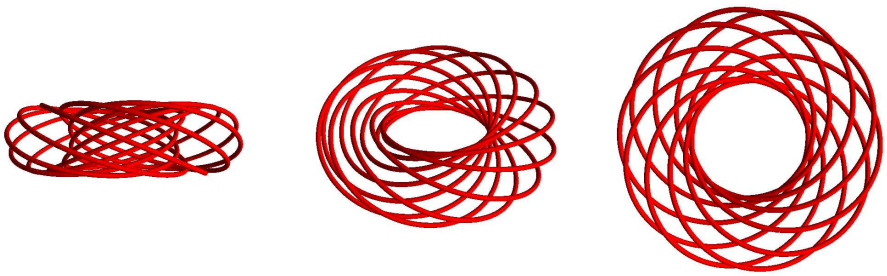

Figure 12: Three views of the tori swept by the red circles corresponding to $k = 1$ in Fig. 11.

Now let us construct the *Hopf map* $\mathrm{S}^3 \xrightarrow{\mathrm{S}^1} \mathrm{S}^2$. To fibre the 3-dimensional sphere S^3 with fibres S^1, we need a map that sends all points from the circle C_μ to a single point. We have already seen such a map – it is the ratio map (14) from $\mathbb{C}^2$ to $\mathbb{C}_\infty$ that was discussed in Sect. 5:

$$\begin{pmatrix} x+iy \\ z+iw \end{pmatrix} \mapsto \frac{x+iy}{z+iw}. \tag{24}$$

It remains to get from $\mathbb{C}_\infty$ to the base space S^2. Recall equation (18) in Sect. 6 that projects the Bloch sphere S^2 to $\mathbb{C}_\infty$. To send S^3 to S^2Thus we have to compose (24) with the inverse of (18) . or the stereographic projection composed with the complex conjugation. First notice that

$$\zeta\overline{\zeta} = \frac{x^2+y^2}{(1-z)^2} = \frac{1-z^2}{(1-z)^2} = \frac{1+z}{1-z}.$$

Then we get (see [5, pp. 11]):

$$x = \frac{\zeta+\overline{\zeta}}{|\zeta|^2+1}, \quad y = i\frac{\zeta-\overline{\zeta}}{|\zeta|^2+1}, \quad z = \frac{|\zeta|^2-1}{|\zeta|^2+1}. \tag{25}$$

One can verify that the S^3 fibration procedure described here is equivalent to the Bloch sphere formalism discussed in Sect. 3, since the composition of (24) and (25) acts on the pure qubit state $|\psi\rangle$ defined in (1) as follows:

$$\begin{pmatrix} \cos\frac{\theta}{2} \\ e^{i\varphi}\sin\frac{\theta}{2} \end{pmatrix} \mapsto e^{-i\varphi}\cot\frac{\theta}{2} \mapsto \begin{pmatrix} \sin\theta\cos\varphi \\ \sin\theta\sin\varphi \\ \cos\theta \end{pmatrix},$$

and the result agrees with the Bloch vector $\vec{r}$ of $|\psi\rangle$ given in (2).

7.3 Generalizations

It turns out that this approach can be generalized to several qubits. The two qubit case is described in [9] (a short summary is also given in [10]), but the three qubit case is considered in [11] (both cases are covered also in [12]).

These generalizations use the Hopf fibrations $\mathrm{S}^7 \xrightarrow{\mathrm{S}^3} \mathrm{S}^4$ and $\mathrm{S}^{15} \xrightarrow{\mathrm{S}^7} \mathrm{S}^8$ of 7-dimensional and 15-dimensional spheres, and can be described using *quaternions*, and *octonions* respectively. The main idea is to rewrite the coordinates of the Bloch vector (2) of the state $|\psi\rangle = \binom{\alpha}{\beta}$ as

$$\begin{cases} x = 2\,\mathrm{Re}(\overline{\alpha}\beta), \\ y = 2\,\mathrm{Im}(\overline{\alpha}\beta), \\ z = |\alpha|^2 - |\beta|^2\,. \end{cases} \tag{26}$$

Then one can use the *Cayley-Dickson construction* to construct larger division algebras and generalize these coordinates for S^4 and S^8.

These generalizations allow to capture the *entanglement* of composite quantum systems (in the sense that separable and entangled states are mapped do different subspaces of the base space). For example, one can iteratively apply the Hopf fibrations to see if a three-qubit state can be decomposed as a product of three one-qubit states. However, it has been proved that there are only four fibrations between spheres:

$$\mathrm{S}^1 \xrightarrow{\mathrm{S}^0} \mathrm{S}^1, \quad \mathrm{S}^3 \xrightarrow{\mathrm{S}^1} \mathrm{S}^2, \quad \mathrm{S}^7 \xrightarrow{\mathrm{S}^3} \mathrm{S}^4, \quad \mathrm{S}^{15} \xrightarrow{\mathrm{S}^7} \mathrm{S}^8.$$

Therefore it is not clear how to generalize this idea further.

References

[1] Bengtsson I., Życzkowski K., Geometry of Quantum States, Cambridge University Press (2006).

[2] Gottesman D., Quantum Error Correction, lecture at *Perimeter Institute* (2007), available at `http://pirsa.org/07010022`.

[3] Mancinska L., Ozols M., Leung D., Ambainis A., Quantum Random Access Codes with Shared Randomness, unpublished, available at `http://home.lanet.lv/~sd20008/RAC/RACs.htm`.

[4] Lee J., Kim C.H., Lee E.K., Kim J., Lee S., Qubit geometry and conformal mapping, *Quantum Information Processing*, **1**, 1-2, 129-134 (2002), `quant-ph/0201014`.

[5] Penrose R., Rindler W., Spinors and Space-Time, Vol. 1, Cambridge University Press (1984).

[6] Conway J.B., Functions of One Complex Variable, 2nd ed., Springer-Verlag (1978).

[7] Lynos D.W., An Elementary Introduction to the Hopf Fibration, *Mathematics Magazine*, Vol. **76**, No. 2., 87-98 (2003).

[8] Thurston W.P., Three-Dimensional Geometry and Topology, Vol. 1, Princeton University Press (1997).

[9] Mosseri R., Dandoloff R., Geometry of entangled states, Bloch spheres and Hopf fibrations, *J. Phys. A: Math. Gen.* **34**, 10243-10252 (2001), `quant-ph/0108137`.

[10] Chruściński D., Geometric Aspects of Quantum Mechanics and Quantum Entanglement, *J. Phys.* **30**, 9-16 (2006).

[11] Bernevig B.A., Chen H., Geometry of the three-qubit state, entanglement and division algebras, *J. Phys. A: Math. Gen.* **36**, 8325-8339 (2003), `quant-ph/0302081`.

[12] Mosseri R., Two-Qubit and Three-Qubit Geometry and Hopf Fibrations, in proceedings of "Topology in Condensed Matter", ed. Monastyrsky M.I., Springer-Verlag (2006), `quant-ph/0310053`.